Tau Aggregation Propensity Engrained in Its Solution State

Neil A. Eschmann,[†] Thanh D. Do,[†] Nichole E. LaPointe,[‡] Joan-Emma Shea,[†] Stuart C. Feinstein,[‡] Michael T. Bowers,[†] Songi Han[†]*

† Department of Chemistry and Biochemistry, ‡ Neuroscience Research Institute and Department of Molecular, Cellular and Developmental Biology, University of California at Santa Barbara, Santa Barbara, California, 93106, United States

SUPPORTING INFORMATION

S1. Comparison of R2/WT and R2/G273C-SL

The mass spectra of R2/WT and R2/G273C-SL in acetate buffer (Figure S1) obtained for fresh samples show only a small difference between the two peptides. It can be seen that, along with the ATD data shown in the paper for R2/WT at m/z = 469 and 705, there is also a dimer contribution (n/z = 2/3) arising at m/z = 940. This peak is very minor in the mass spectrum for R2/G273C-SL. This difference between the two peptides is considered insignificant as it only suggests that the dimer population for the R2/WT peptide is separated into two charge states (+3 and +4) as opposed to only one in R2/G273C-SL. Also, it should be noted that there are several more unresolved peaks in the mass spectrum of the peptide in sodium phosphate buffer. This observation is due to phosphate buffer ions forming adducts with the parent peptide, leading to the presence of several new peaks with different m/z values. Therefore, it is concluded that there is no significant difference between the R2/WT peptide and the mutated form R2/G273C-SL and will treat further data such that observations observed with R2/G273C-SL is a good model for how R2/WT behaves.

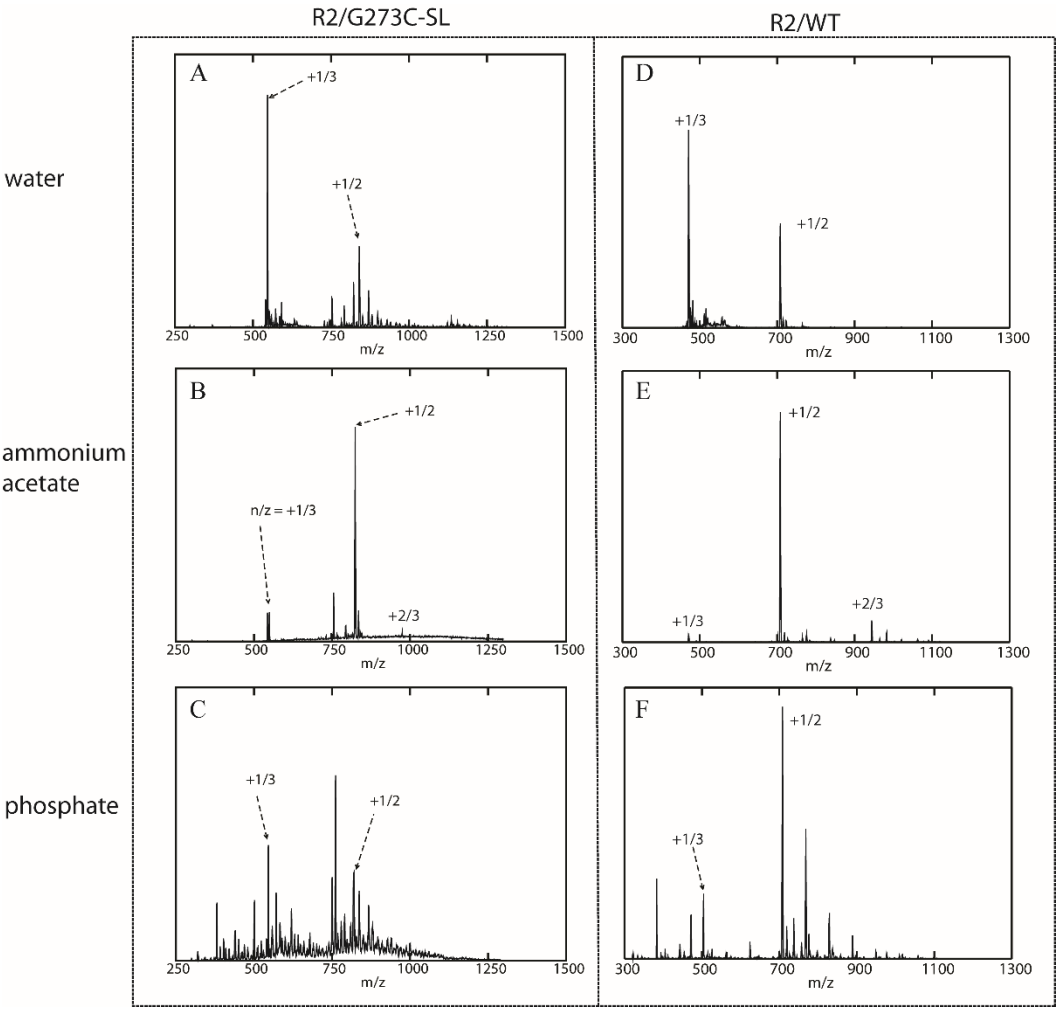

Figure S1 ESI-q-mass spectra of R2/G273C-SL and R2/WT dissolved in water (A and D respectively), 20 mM ammonium acetate buffer pH = 7.0 (B and E respectively) and 20 mM phosphate buffer pH = 7.0 (C and F respectively).

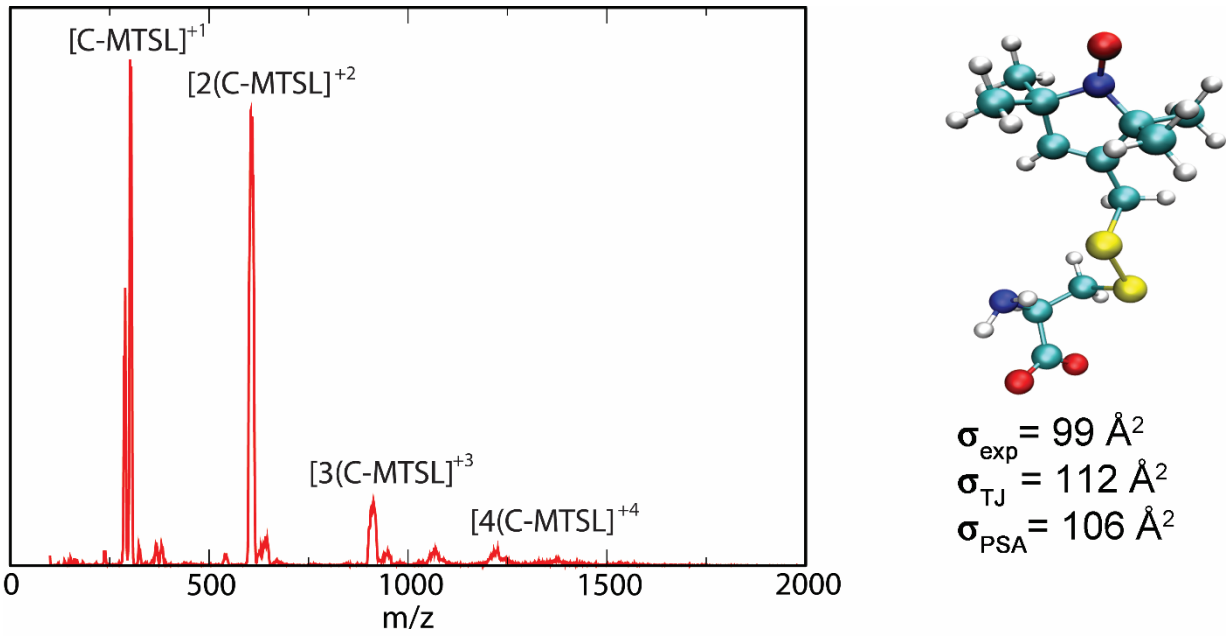

Figure S2. ESI-q-mass spectrum of 500 µM C-MTSL in water. The cross section of [C-MTSL]$^{1+}$ was obtained from measuring the ATDs at 306 *m/z*.

Theoretical structure of C-MTSL was obtained in two stages. In the first stage, B3LYP/ 6-31G** calculation using ROHF wavefunction available from the GAMESS package[1-2] was performed on the C-MTSL system in which the two termini are blocked with two methyl groups so that the correct partial charge on the MTSL probe could be obtained. In the second stage, the optimized geometry and partial changes are input in a two-stage charge fitting using the R.E.D. (RESP ESP charge Derive) package[3] so that the whole unit is a modified amino acid with consistent partial change and geometry.

Theoretical cross section was obtained from the trajectory method (TJ) available from the Mobcal package[4-5] and the projected approximation method (PSA) available at http://luschka.bic.ucsb.edu:8080/WebPSA/.[6-7] Because both of the methods do not treat the structure as a radical, the obtained cross section would neglect any potential interactions between the radical with the buffer gas, yielding the predicted cross section for a protonated system.

Discussion on n/z = 1/3 peak of the R2/G273C-SL:

The ATD of R2/G273C-SL peptide (Figure 3C, main text) displays more complex features than the ATD of the WT (*m/z* = 469, Figure 3A). The *n/z* = 1/3 ATD of the R2/G273C-SL peptide contains a dominant feature with a cross section very similar to that of the R2/WT (σ = 338 Å^2 vs. 336 Å^2) if assigned to be a monomer. This is unexpected as adding a MTSL label should significantly increase the cross section assuming the WT and R2/G273C-SL peptide adopt similar monomer conformations. A possible explanation to assigning this feature as a monomer is that the *m/z*=546 population may contain both protonated and radical monomers, in which the latter species interacts more strongly with a buffer gas resulting in a shorter mobility. A previous IMS study by Laakia et al showed that both 2,6-Di-tert-butyl-4-pyridine and 2,6-Di-tert-butyl-4-methylpyridine radical ions $[M]^{+\cdot}$ have lower mobilities than protonated $[M+H]^+$ (the *m/z* difference between the two types of species is 1 *m/z* or less).[8] Two additional experiments on the cysteine-MTSL complex were performed to investigate the effect of MTSL radical ion on the cross section. In the first experiment, a combination of IMS and DFT calculation reveals that the cysteine-MTSL (see Figure S2) has a smaller experimental collision cross section (σ = 99 Å^2) than theoretical prediction (σ_{av} = 109 Å^2) suggesting the presence of the radical reduces the cross section of the ion. In the second experiment, we investigate the same mass spectral peaks of two additional peptides, namely R2/I278C-SL and R2/L284C-SL. In the first peptide, the probe is placed in the middle region and is less exposed than for R2/G273C-SL and R2/L284C-SL (the MTSL probe is at the N and C-termini of these two peptides, respectively). Ion-mobility studies of the *n/z* = 1/3 mass spectral peaks reveal that the shortest arrival time feature is dominant in the cases of R2/G273C-SL and R2/L284C-SL, but its intensity is significantly reduced for the

R2/I278C-SL peptide (see Figure S3). Therefore, we assign this feature as a monomer rather than a dimer.

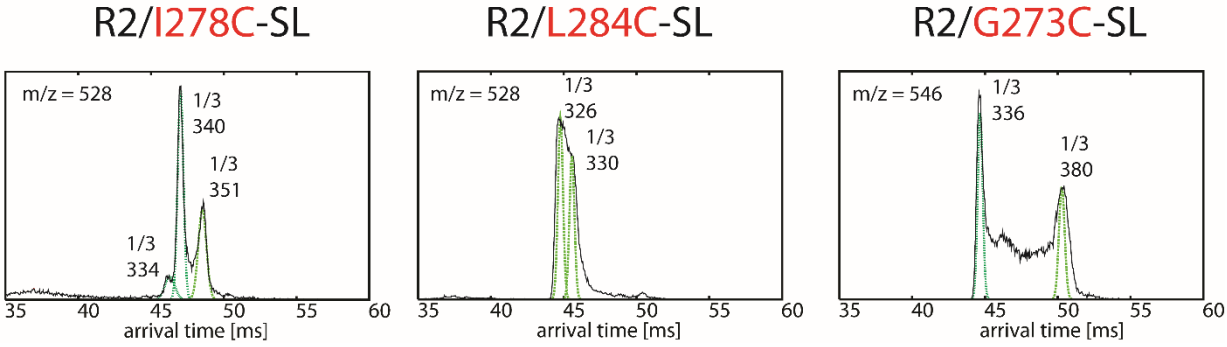

Figure S3. Representative ATDs of the *n/z* = 1/3 mass spectral peaks of the three mutants. Each feature is annotated with *n/z* and experimental cross section (σ, Å^2)

S2. Effect of Osmolytes on Oligomeric State and Aggregation Propensity

Figure S4 shows EPR spectra of R2/G273C-SL before aggregation in the absence of osmolytes and in the presence of 4.4 M urea or 2 M TMAO. It can be seen there is very little change in the EPR spectrum when 4.4 M urea is added compared to that of the peptide dissolved only in ammonium acetate buffer suggesting the spin label remains relatively mobile. However, when the peptide is dissolved in 2 M TMAO, we see a significant drop in the EPR spectrum which is likely caused by dipolar broadening arising from the formation of oligomers and aggregates.

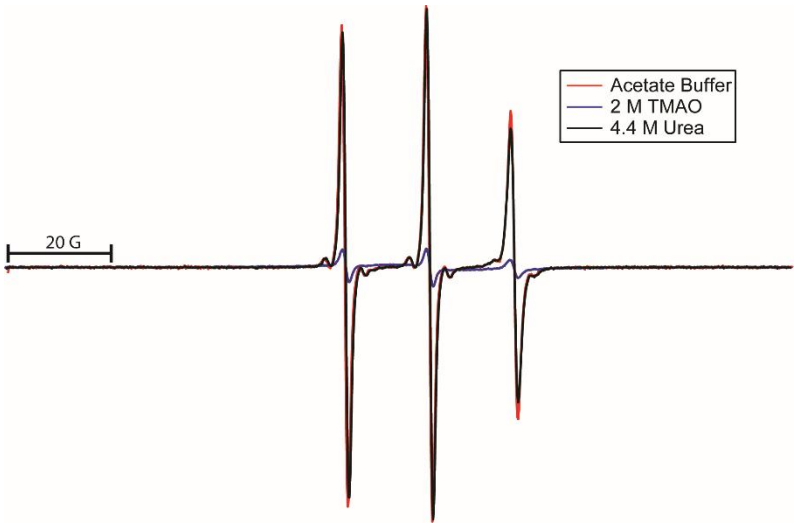

Figure S4. EPR of R2/G273C-SL before heparin addition in 20 mM ammonium acetate buffer (pH = 7.0) in the presence or absence of 2 M TMAO or 4.4 M urea.

S3. Buffers Modulate R2/G273C-SL Oligomer Formation

Here we report on the effect of dissolving R2/G273C-SL in different buffers including ammonium acetate buffer, sodium phosphate buffer, and water. We used IM-MS, ODNP, EPR, TEM, and ThT assay to characterize the differences between the solvents. Before the addition of heparin, EPR shows the spin label is mobile and solvent exposed in all three solvent conditions as depicted by the sharp lineshape shown in figure S5.

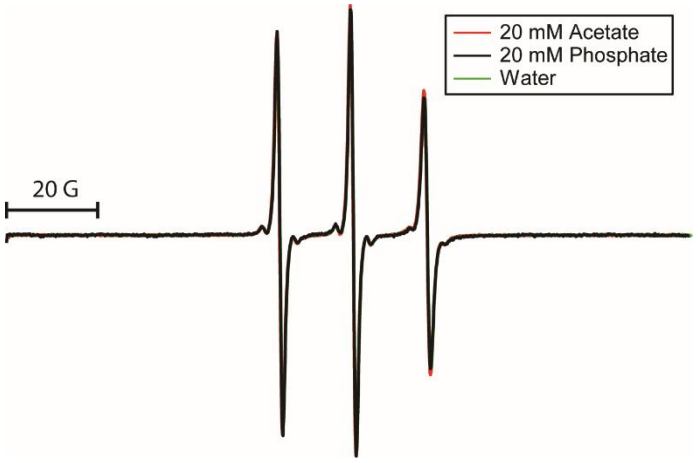

Figure S5. EPR of R2/G273C-SL dissolved in either pure water, 20 mM ammonium acetate buffer (pH = 7.0), or 20 mM phosphate buffer (pH = 7.0) before the addition of heparin.

As seen in Figure S1, the mass spectrum for each of the buffer conditions before adding heparin is very similar. In comparing the spin labeled peptide, there is only a slight difference in the fact that for water and sodium phosphate buffer, the peak corresponding to n/z = 1/3 is more abundant than n/z = 1/2 whereas the opposite is true for acetate buffer. Figure S6 shows the ATD data at n/z = 1/3 and 1/2 for all three solvent conditions. It can be seen that for R2/G273C-SL there is a slightly different distribution of conformations for n/z = 1/3. More importantly, it can be noticed that ammonium acetate buffer and sodium phosphate buffer appear to stabilize the extended (native) conformation of the peptide. On the other hand, for the ATD of n/z = 1/2, the peptide dissolved in water and ammonium acetate buffer behave very similarly such that they both contain monomer with a +2 charge as well as a more abundant dimer peak with a +4 charge, while the peptide dissolved in sodium phosphate buffer only has a dimer population with a +4 charge.

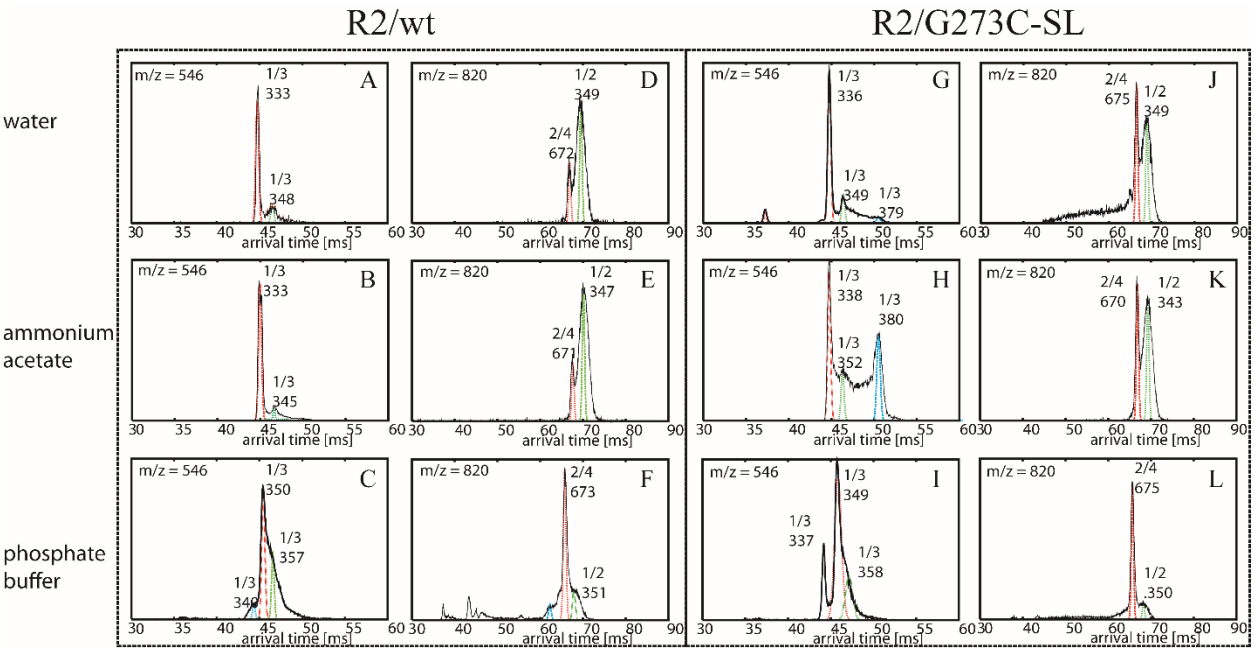

Figure S6. Representative ATDs at n/z = 1/3 and n/z = 1/2 of R2/G273C-SL. Solvents appear to have a small effect on the oligomer distributions of R2/wt in which the +4 extended dimer is more favored in buffer than in water. Similar effects are observed in the mutant, where the extended (more native) +3 monomers are preserved and the population of the +4 extended dimer is higher in buffer than in water.

There is a clearer difference between the three solvent conditions upon the addition of heparin to aggregate the peptide. Data for the peptide with heparin dissolved in ammonium acetate buffer is shown in Figure 6 (in the main text). Figure S7 shows R2/G273C-SL with heparin dissolved in water and sodium phosphate buffer. When the peptide is dissolved in water and induced with heparin, the signature of the peptide appears at t = 0 and does not change through 2 hours. Furthermore, ATD data shows no shift in oligomeric state upon aggregation. The data suggest a slow kinetics of aggregation in this condition. In the presence of sodium phosphate buffer, the mass spectrum shows a monomer peak as a signature of the peptide as well as a rising baseline which is indicative of the formation of aggregates. The signature peak

remains after 30 minutes but after 1 hour, the peak completely disappears and only unresolved large oligomers are detected at high *m/z* values in the mass spectra. The ATDs under this condition populate multiple features as a result of adduct ions falling apart, leading to the formation of additional features with different mobility. Hence we cannot unambiguously assign any new features to new oligomers. However, the overall ATDs suggest the protein signatures (the features corresponding to monomer and dimer at $n/z = 1/2$) quickly disappear as a result of fast aggregation kinetics. Overall, IM-MS data shows that R2/G273C-SL dissolved in ammonium acetate buffer and sodium phosphate aggregates very well while the same peptide dissolved in water appears to not form any aggregates at 50 μM concentration. Furthermore, the rate of aggregation in sodium phosphate buffer appears to be accelerated compared to ammonium acetate buffer, in that aggregates are observed in sodium phosphate buffer immediately after heparin addition, whereas aggregates are not observed in ammonium acetate buffer until 1.5 hours after heparin addition.

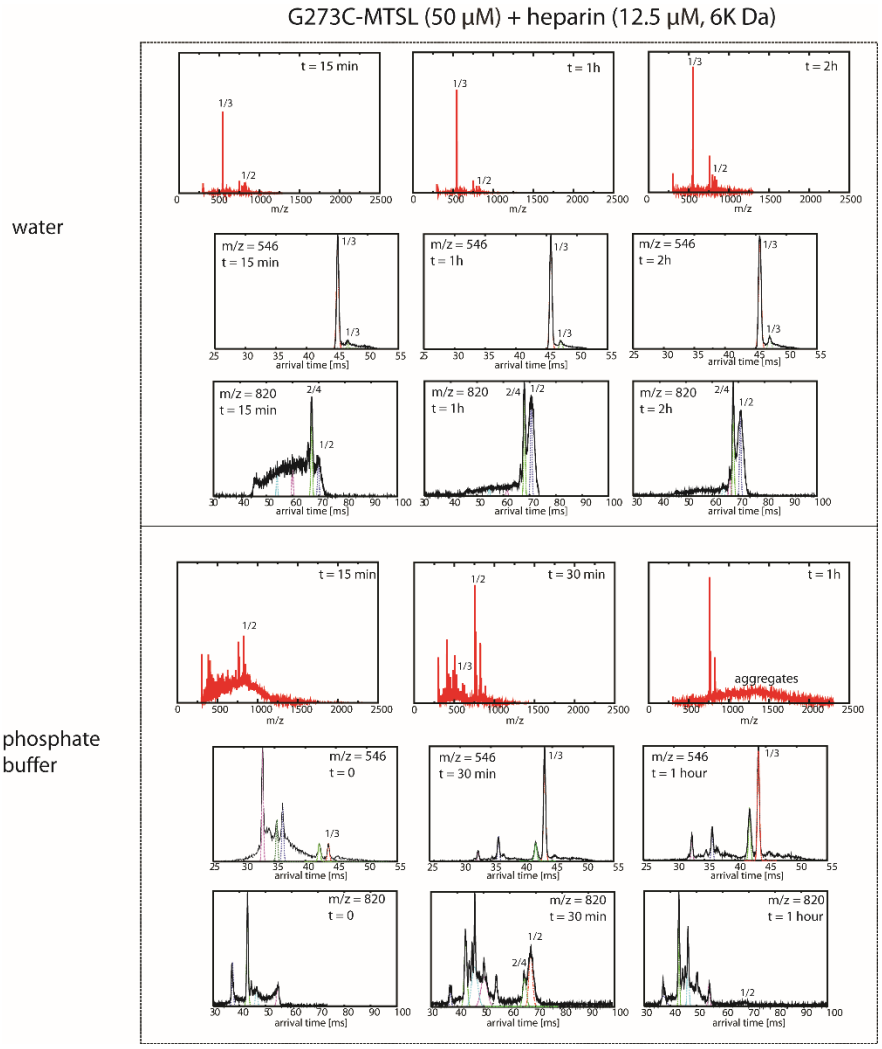

Figure S7. ESI-q-mass spectra and representative ATDs of 50 µM R2/G273C-SL in the presence of 12.5 µM 6 kDa heparin in water and phosphate buffer (pH = 7.0). The aggregation occurs instantly in phosphate buffer but slows down in water. The observation of weak aggregation in water is consistent with our previous study on R2/WT, which shows similar results when comparing water with acetate buffer.

Table S1 shows ODNP reference measurements of 4-hydroxy Tempo in a variety of different buffers which are used in this paper. Measurements for acetate vs. water vs. phosphate show no discernable differences in $k\sigma$, which means that any major changes in $k\sigma$ for R2/G273C-

SL are strictly due to changes in peptide conformation/population. Reference measurements in the presence of urea and TMAO are much slower as expected, due to increased solvent viscosity.

Buffer Condition	Acetate	Water	Phosphate	Urea	TMAO
$k\sigma$	56.6 ± 0.5 $s^{-1}M^{-1}$	63.9 ± 0.4 $s^{-1}M^{-1}$	67.2 ± 0.3 $s^{-1}M^{-1}$	33.4 ± 0.4 $s^{-1}M^{-1}$	31.5 ± 0.4 $s^{-1}M^{-1}$

Table S1. ODNP reference measurements of 4-hydroxy Tempo dissolved in 20 mM ammonium acetate buffer (pH = 7.0), 20 mM phosphate buffer (pH = 7.0) or pure water. Also, reference measurements are shown for added osmolytes which are dissolved in 20 mM ammonium acetate buffer (pH = 7.0) and either 4.4 M urea or 2 M TMAO.

REFERENCES

1. Schmidt, M. W.; Baldridge, K. K.; Boatz, J. A.; Elbert, S. T.; Gordon, M. S.; Jensen, J. H.; Koseki, S.; Matsunaga, N.; Nguyen, K. A.; Su, S., et al. General Atomic and Molecular Electronic Structure System. *J. Comput. Chem.* **1993,** *14*, 1347-1363.

2. Gordon, M. S.; Schmidt, M. W. Advances in Electronic Structure Theory: Gamess a Decade Later. *Theory and Applications of Computational Chemistry: The First Forty Years* **2005**, 1167-1189.

3. Dupradeau, F.-Y.; Pigache, A.; Zaffran, T.; Savineau, C.; Lelong, R.; Grivel, N.; Lelong, D.; Rosanski, W.; Cieplak, P. The R.E.D. Tools: Advances in Resp and Esp Charge Derivation and Force Field Library Building. *Phys. Chem. Chem. Phys.* **2010,** *12*, 7821-7839.

4. Shvartsburg, A. A.; Liu, B.; Jarrold, M. F.; Ho, K.-M. Modeling Ionic Mobilities by Scattering on Electronic Density Isosurfaces: Application to Silicon Cluster Anions. *J. Chem. Phys.* **2000,** *112*, 4517-4526.

5. Mesleh, M. F.; Hunter, J. M.; Shvartsburg, A. A.; Schatz, G. C.; Jarrold, M. F. Structural Information from Ion Mobility Measurements: Effects of the Long-Range Potential. *J. Phys. Chem.* **1996,** *100*, 16082-16086.

6. Bleiholder, C.; Contreras, S.; Do, T. D.; Bowers, M. T. A Novel Projection Approximation Algorithm for the Fast and Accurate Computation of Molecular Collision Cross Sections (Ii). Model Parameterization and Definition of Empirical Shape Factors for Proteins. *Int. J. Mass. Spectrom.* **2013,** *345–347*, 89-96.

7. Bleiholder, C.; Wyttenbach, T.; Bowers, M. T. A Novel Projection Approximation Algorithm for the Fast and Accurate Computation of Molecular Collision Cross Sections (I). Method. *Int. J. Mass. Spectrom.* **2011,** *308*, 1-10.

8. Laakia, J.; Adamov, A.; Jussila, M.; Pedersen, C.; Sysoev, A.; Kotiaho, T. Separation of Different Ion Structures in Atmospheric Pressure Photoionization-Ion Mobility Spectrometry-Mass Spectrometry (Appi-Ims-Ms). *J. Am. Soc. Mass. Spectrom.* **2010,** *21*, 1565-1572.